Complex frequencies of a massless scalar field in loop quantum black hole spacetime*

Chen Ju-Hua(陈菊华)† and Wang Yong-Jiu(王永久)

College of Physics and Information Science, Key Laboratory of Low Dimensional Quantum Structures and Quantum Control at the Ministry of Education, Hunan Normal University, Changsha 410081, *China*

(Received 23 July 2010; revised manuscript received 19 August 2010)

Recently, considerable progress has been made in understanding the early universe by loop quantum cosmology. Modesto *et al.* investigated the loop quantum black hole (LQBH)using improved semiclassical analysis and they found that the LQBH has two horizons, an event horizon and a Cauchy horizon, just like the Reissner–Nordström black hole. This paper focuses on the dynamical evolution of a massless scalar wave in the LQBH background. By investigating the relation between the complex frequencies of the massless scalar field and the LQBH parameters using the numerical method, we find that the polymeric parameter P makes the massless scalar field decay more quickly and makes the ground scalar wave oscillate slowly. However, the polymeric parameter P causes the frequency of the high harmonic massless scalar wave to shift according to its value. We also find that the loop quantum gravity area gap parameter a_0 causes the massless scalar field to decay more slowly and makes the period of the massless scalar field wave become longer. In the complex ω plane, the frequency curves move counterclockwise when the polymeric parameter P increases and this spiral effect is more obvious for a higher harmonic scalar wave.

Keywords: complex frequencies, massless scalar field, loop quantum black hole spacetime

PACS: 04.20.–q, 04.80.–y **DOI:** 10.1088/1674-1056/20/3/030401

1. Introduction

Loop quantum gravity (LQG)[1−4] is a fundamental quantum geometric theory that reconciles general relativity and quantum mechanics at the Planck scale, and we expect that this theory could resolve the classical singularity problems of general relativity. The applications of LQG technology are to solve two kinds of classical singularity problems. One is to solve the initial singularity problem of early universe,[5,6] the other is to solve the black hole singularity problem by using tools and ideas developed in full LQG.[7−9] A simplified framework, which uses the minisuperspace approximation, has been shown to resolve the initial singularity problem.[4] A black hole metric (the loop black hole (LBH))[10] was obtained dynamically inside the homogeneous region (that is inside the horizon where space is homogeneous but not static). The outside of its horizon shows that one can reduce the two free parameters by identifying the minimum area presented in the solution with the minimum area of LQG. The thermodynamic properties[10,11] and the dynamical aspects of the collapse and the evaporation[12] of these self-dual black holes have been studied previously. These black hole spacetimes have also been investigated in a midi-superspace reduction of LQG.[13]

The quasinormal modes(QNMs),[14] which depend on black hole parameters, are of great importance in gravitational-wave astrophysics and might be observed in existing or advanced gravitational-wave detectors. Furthermore, black holes are often used as a testing ground for ideas in quantum gravity and their QNMs are obvious candidates for interpretation in terms of quantum levels.[15] Meanwhile, the investigation on QNMs may lead to a deep understanding of the thermodynamic properties of black holes in LQG,[16,17] as well as the QNMs of anti-de Sitter black holes, which have a direction interpretation in terms of the dual conformal field theory.[18,19] Therefore, in the past few decades there have been a lot of authors who have focused on the QNMs of matter fields in different black hole backgrounds, such as the QNMs of black holes in anti-de Sitter space,[20−22] the Dirac field QNMs[23−25] and the scalar field QNMs[26−29] in different backgrounds. Recently, some scholars have investigated the effect of dark energy and dark

*Project supported Project supported by the National Natural Science Foundation of China (Grant No. 10873004), the Program for Excellent Talents at Hunan Normal University, China, the National Basic Research Program of China (Grant No. 2010CB832803), the Key Program of the National Natural Science Foundation of China (Grant No. 10935013), the Construct Program of the National Key Discipline, and the Program for Changjiang Scholars and the Innovative Research Team in University, China (Grant No. IRT0964).

†Corresponding author. E-mail: jhchen@hunnu.edu.cn

© 2011 Chinese Physical Society and IOP Publishing Ltd

matter on QNMs[30−43], and some others have extended the investigation of QNMs to higher dimensional spacetimes.[44−48]

Recently, Modesto *et al.*[10,13] concentrated their attention on the space-time structure of the loop quantum black hole (LQBH) using improved semiclassical analysis, i.e., the conservative approach of the constant polymeric parameter. They found that the LQBH has two horizons, an event horizon and a Cauchy horizon, and the LQBH has improved stability over classical two-horizon black holes, such as the Reissner–Nordström black hole (RNBH). From these references, we can see some similarities in the properties of space-time structure in the LQBH and RNBH. It is well known that some authors[49−51] have investigated the different fields evolution in the RNBH background. Therefore, it is interesting to study the evolution of the massless scalar field in LQBH spacetime. In this paper, we plan to investigate whether there are some similar properties in dynamical evolution in these two kinds of spacetime background.

2. Dynamical evolution of massless scalar field in LQBH spacetime

The spherically symmetric solution corrected by quantum gravitation[10,52] can take the following form:

$$\begin{aligned} \mathrm{d}s^2 &= -A(r)\mathrm{d}t^2 + B^{-1}(r)\mathrm{d}r^2 \\ &\quad + C(r)(\mathrm{d}\theta^2 + \sin^2\theta\mathrm{d}\varphi), \end{aligned} \tag{1}$$

where

$$A(r) = \frac{(r-2m)(r-2mP^2)(r+2mP)^2}{r^4+a_0^2}, \tag{2}$$

$$B(r) = \frac{(r-2m)(r-2mP^2)r^4}{(r+2mP)^2(r^4+a_0^2)}, \tag{3}$$

$$C(r) = r^2 + \frac{a_0^2}{r^2}. \tag{4}$$

Here, the polymeric parameter $P = (\sqrt{1+\epsilon^2}-1)/(\sqrt{1+\epsilon^2}+1)$, where $\epsilon = \delta\gamma$ is the product of the Immirzi parameter γ and the polymeric quantity δ. The quantum gravitational corrections become relevant only when the curvature is in the Planckian regime, corresponding to $\epsilon < 1$. The parameter a_0 is the area gap of LQG.

The general perturbation equation for the massless scalar field in curved spacetime is given by

$$\frac{1}{\sqrt{-g}}\partial_\mu(\sqrt{-g}g^{\mu\nu}\partial_\nu)\psi = 0, \tag{5}$$

where ψ is the massless scalar field.

Because of the spherically symmetric property of LQBH spacetime, we can divide the wave solution ψ into the form $\psi = (\mathrm{e}^{-\mathrm{i}\omega t}\Phi(r)/r)Y(\theta,\varphi)$, where $Y(\theta,\varphi)$ is the spherical harmonic function. Substituting Eq. (1) into Eq. (5), we obtain the radial perturbation equation

$$\begin{aligned} &\frac{\sqrt{A(r)B(r)}}{C(r)}\frac{\partial}{\partial r}\left[C(r)\sqrt{A(r)B(r)}\frac{\partial\Phi(r)}{\partial r}\right] \\ &= \left[l(l+1)\frac{A(r)}{C(r)} - \omega^2\right]\Phi(r), \end{aligned} \tag{6}$$

If we introduce the following tortoise coordinate:

$$\frac{\mathrm{d}r_*}{\mathrm{d}r} = \frac{1}{\sqrt{A(r)B(r)}}, \tag{7}$$

then the radial perturbation Eq. (6) can be simplified to

$$\frac{\mathrm{d}^2\Phi(r)}{\mathrm{d}r_*^2} + [\omega^2 - V(r)]\Phi(r) = 0, \tag{8}$$

where

$$\begin{aligned} V(r) &= l(l+1)\frac{A(r)}{C(r)} + \frac{1}{2}\sqrt{\frac{A(r)B(r)}{C(r)}} \\ &\quad \times\left[\frac{\partial}{\partial r}\left(\sqrt{\frac{A(r)B(r)}{C(r)}}\frac{\partial C(r)}{\partial r}\right)\right]. \end{aligned} \tag{9}$$

It is obvious that the effective potential V depends on the radial coordinate r for fixed parameters of angular quantum number l, mass m, the polymeric parameter P and the LQG area gap a_0, respectively. Because Eq. (9) is so complicated, we cannot straightly see its r-dependence properties for fixed parameters. Figures 1–3 give the behaviour of the effective potential versus r for the LQBH for fixed parameters. Figure 1 and Fig. 4(a) show the variation of the effective potential and its peak points r_p with respect to the polymeric parameter P. From these two figures we find that the peak values of the potential barrier get higher and the location of the peak ($r = r_\mathrm{p}$) moves forward to the right side when the polymeric parameter P increases. In Fig. 2 and Fig. 4(b) we provide the variation of the effective potential and its peak point r_p with respect to the LQG area gap a_0. From these two figures we can find that the peak value of the potential barrier becomes lower, which is different from the above case, but the location of the peak ($r = r_\mathrm{p}$) also moves forward to the right side when the LQG area gap a_0 increases. However, from Fig. 3 we can see that the peak value of potential barrier gets higher

and the location of the peak point ($r = r_{\rm p}$) moves forward to the right side when the angular quantum number l increases.

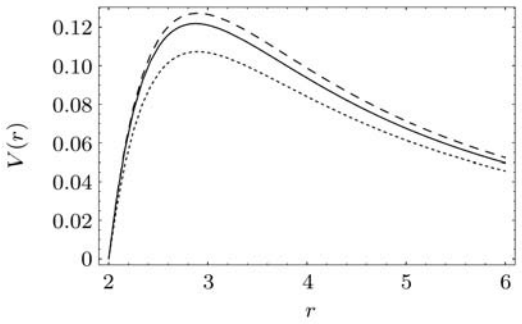


Fig. 1. The behaviour of the effective potential $V(r)$ versus r for the LQBH with fixed parameters $l = 1, m = 1, a_0 = \sqrt{3}/2$ and the polymeric parameter $P = 0.1$ (dotted line), 0.3 (solid line), 0.5 (dashed line).

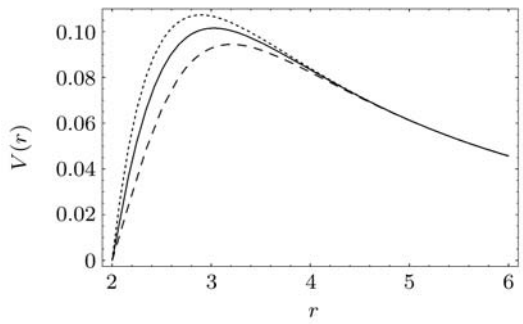


Fig. 2. The behaviour of the effective potential $V(r)$ versus r for the LQBH with fixed parameters $l = 1, m = 1, P = 0.1$ and the minimum area gap constant $a_0 = \sqrt{3}/2$ (dotted line), $\sqrt{15}/2$ (solid line), $\sqrt{35}/2$ (dashed line).

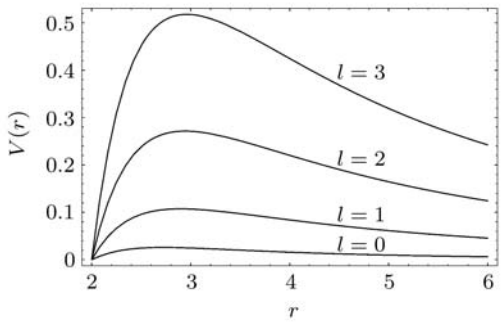
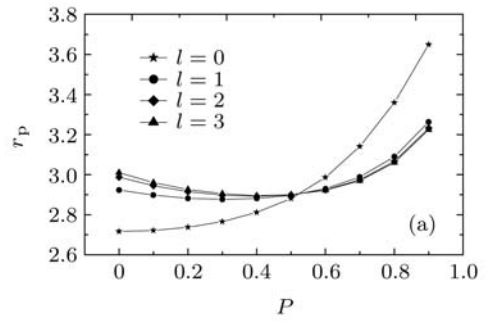


Fig. 3. The behaviour of the effective potential $V(r)$ versus r for the LQBH with by fixed parameters $m = 1, a_0 = \sqrt{3}/2, P = 0.1$ and the angular quantum number $l = 0, 1, 2, 3$ (from bottom to top).



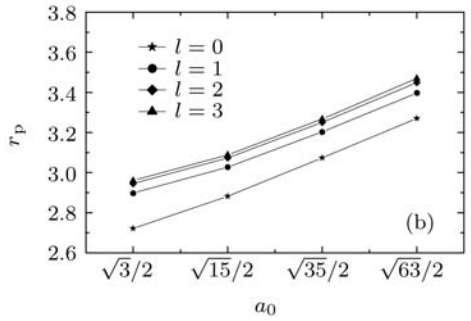


Fig. 4. The peak point ($r = r_{\rm p}$) of the effective potential versus the parameters of the LQBH for different angular quantum numbers. (a) corresponds to Fig. 1 and (b) corresponds to Fig. 2.

3. Simulations on complex frequencies of massless scalar field

From the effective potential $V(r)$, i.e., Eq. (9) and Figs. 1 and 2, we find that the complex frequencies depend on the polymeric parameter P and the LQG area gap a_0. In this paper, we investigate the relations between the complex frequencies and the polymeric parameter P and the LQG area gap a_0 in detail. In order to evaluate the complex frequencies of the massless scalar field in LQBH spacetime (1), we use the third-order WKB approximation, a numerical method introduced by Schutz, Will and Iyer.[53–55] This method has been extensively used to evaluate the complex frequencies of various black holes due to its considerable accuracy for lower-lying modes. In this approximate method, the formula for the complex frequency ω is

$$\omega^2 = [V_0 + (-2V''_0)^{1/2}\Lambda] - {\rm i}(n+\frac{1}{2})(-2V''_0)^{1/2}(1+\Omega), \quad (10)$$

where

$$\Lambda = \frac{1}{(-2V''_0)^{1/2}}\left\{\frac{1}{8}\left(\frac{V_0^{(4)}}{V''_0}\right)\left(\frac{1}{4}+N^2\right) - \frac{1}{288}\left(\frac{V'''_0}{V''_0}\right)^2(7+60N^2)\right\}, \quad (11)$$

$$\Omega = \frac{1}{(-2V''_0)^{1/2}}\left\{\frac{5}{6912}\left(\frac{V'''_0}{V''_0}\right)^4(77+188N^2) - \frac{1}{384}\left(\frac{V'''^2_0 V_0^{(4)}}{V''^3_0}\right)(51+100N^2) + \frac{1}{2304}\left(\frac{V_0^{(4)}}{V''_0}\right)^2(67+68N^2)\right.$$

$$+\frac{1}{288}\left(\frac{V'''_0 V_0^{(5)}}{V''^2_0}\right)(19+28N^2)$$
$$-\frac{1}{288}\left(\frac{V_0^{(6)}}{V''_0}\right)(5+4N^2)\Bigg\}, \qquad (12)$$

and

$$N=n+\frac{1}{2}, \qquad V_0^{(s)}=\left.\frac{\mathrm{d}^s V}{\mathrm{d}r_*^s}\right|_{r_*=r_*(r_\mathrm{p})}, \qquad (13)$$

where n is the overtone number and r_p is the value of polar coordinate r corresponding to the peak of the effective potential (9). Substituting the effective potential (9) into the formula above, we can obtain the complex frequencies of the massless scalar field in self-dual black hole spacetime. Figure 5 and Table 1 show the real and imaginary complex frequency parts of the massless scalar field with the variation of the polymeric parameter P and angular quantum number l. By analysing these data and curves, we can find that, when the polymeric parameter P increases, the real part of the ground complex frequency of the massless scalar field decreases, but the imaginary part of the complex frequency of the massless scalar field increases, which means that the polymeric parameter P causes the massless scalar field to decay more quickly and makes the scalar oscillate slowly. However, it is more complicated for the harmonic scalar wave. i.e., high angular quantum numbers l. See $l=2,3$ curves in Fig. 5, the real parts of the complex frequency increase first and then decrease as the polymeric parameter P increases. This means that the polymeric parameter P makes the frequency of the high harmonic massless scalar wave shift blue first and then red.

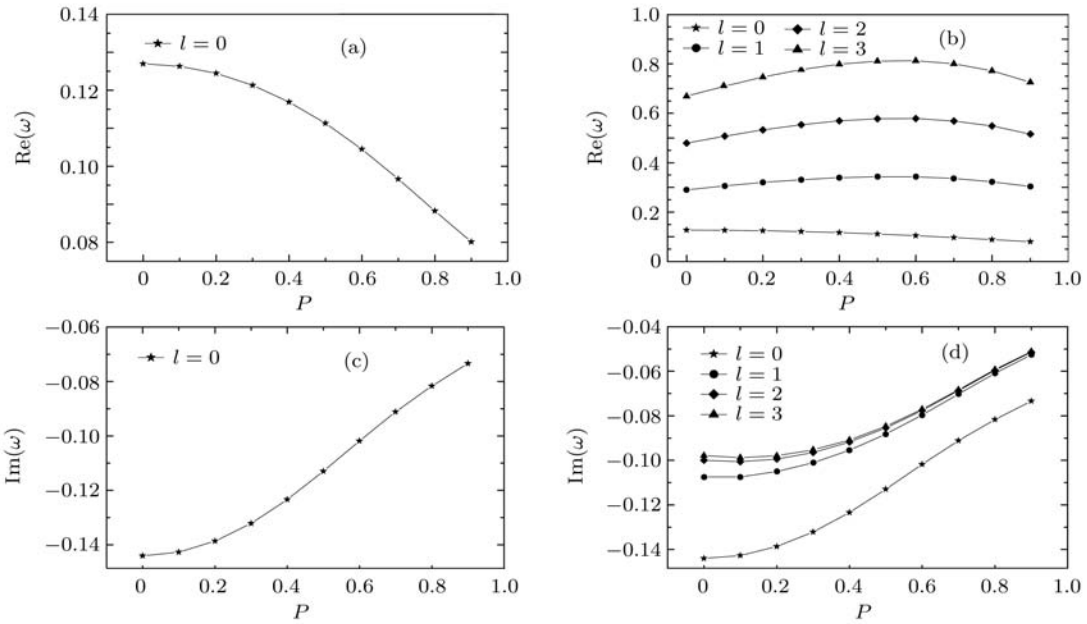


Fig. 5. Variation of real parts Re(ω) ((a), (b)) and imaginary parts Im(ω) ((c),(d)) of complex frequencies of the massless scalar field in the LQBH spacetime with parameters $m=1, a_0=\sqrt{3}/2$.

Table 1. Complex frequencies of the massless scalar field in LQBH spacetime with parameters $m=1, a_0=\sqrt{3}/2$ and $n=0$.

P	ω ($l=0$)	ω ($l=1$)	ω ($l=2$)	ω ($l=3$)
0	0.12696–0.14404i	0.29041–0.10738i	0.47909–0.09994i	0.66913–0.09784i
0.1	0.12633–0.14269i	0.30612–0.10713i	0.50775–0.10060i	0.71019–0.09876i
0.2	0.12443–0.13867i	0.31986–0.10501i	0.53303–0.09925i	0.74646–0.09791i
0.3	0.12129–0.13213i	0.33106–0.10108i	0.55390–0.09652i	0.77650–0.09526i
0.4	0.11692–0.12337i	0.33907–0.09541i	0.56925–0.09180i	0.79872–0.09082i
0.5	0.11131–0.11297i	0.34315–0.08819i	0.57782–0.08542i	0.81137–0.08468i
0.6	0.10449–0.10185i	0.34246–0.07965i	0.57821–0.07758i	0.81246–0.07704i
0.7	0.09662–0.09115i	0.33606–0.07028i	0.56885–0.06870i	0.79981–0.06829i
0.8	0.08825–0.08165i	0.32310–0.06086i	0.54826–0.05956i	0.77134–0.05923i
0.9	0.08011–0.07340i	0.30332–0.05260i	0.51579–0.05141i	0.72606–0.05111i

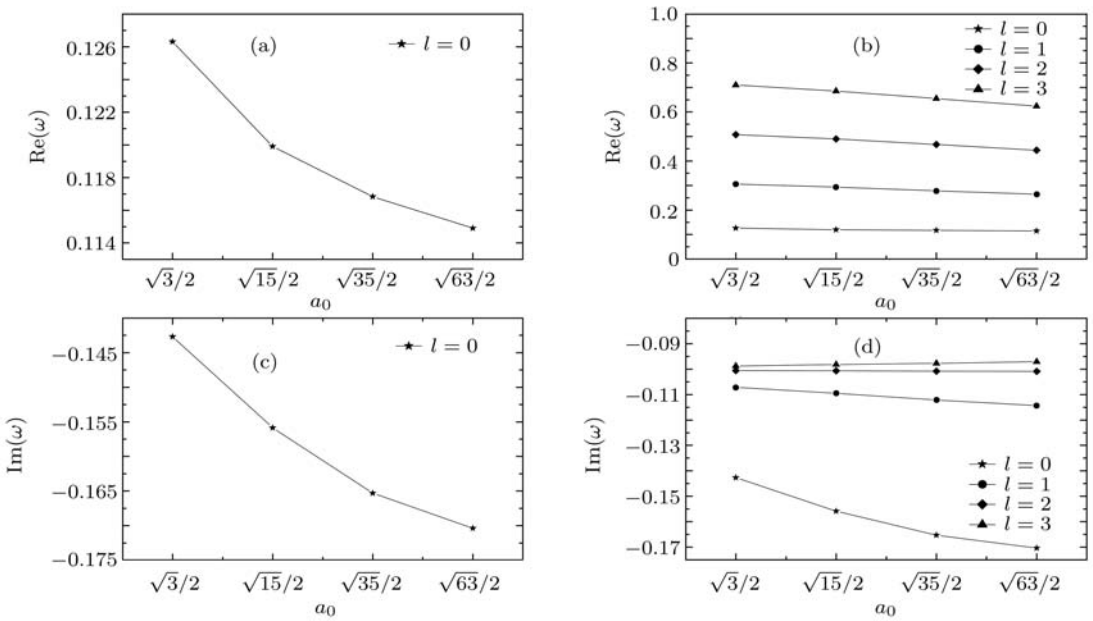


Fig. 6. Variation of the real parts Re(ω) ((a), (b)) and the imaginary parts Im(ω) ((c),(d)) of complex frequencies of the massless scalar field in LQBH spacetime with parameters $m = 1, P = 0.1$.

Table 2. Complex frequencies of the scalar field in the LQBH spacetime with parameters $m = 1, P = 0.1$ and $n = 0$.

a_0	ω ($l = 0$)	ω ($l = 1$)	ω ($l = 2$)	ω ($l = 3$)
$\sqrt{3}/2$	0.12632–0.14269i	0.30612–0.10713i	0.50775–0.10060i	0.71020–0.09876i
$\sqrt{15}/2$	0.11991–0.15586i	0.29350–0.10948i	0.48973–0.10064i	0.68580–0.09820i
$\sqrt{35}/2$	0.11683–0.16532i	0.27857–0.11216i	0.46716–0.10082i	0.65500–0.09768i
$\sqrt{63}/2$	0.11490–0.17039i	0.26410–0.11435i	0.44436–0.10086i	0.62359–0.09710i

Figure 6 and Table 2 show the variation between the complex frequency of the massless scalar field and the LQG area gap a_0 and angular quantum number l. We find that, when the LQG area gap a_0 increases, the real (imaginary) parts of complex frequency of the massless scalar field decrease, which means that the LQG area gap parameter a_0 makes the massless scalar field decay more slowly and makes the period of the massless scalar field wave become longer.

In Fig. 7, we show the effects of the polymeric parameter P on the massless scalar wave evolution in the complex ω plane for different angular quantum numbers $l = 1, 2, 3$. We find that the frequency curves move counterclockwise as the polymeric parameter P increases in the complex ω plane. At the same time, this spiral effect is more obvious for a higher harmonic scalar wave. Jing,[49] Shu and Shen[50] have also found a similar property in a Dirac field in an RNBH background. This means that the LQBH not only has a similar spacetime structure, such as two horizons (event horizon and Cauchy horizon),[10,13] but also a dynamical evolution like the RNBH.

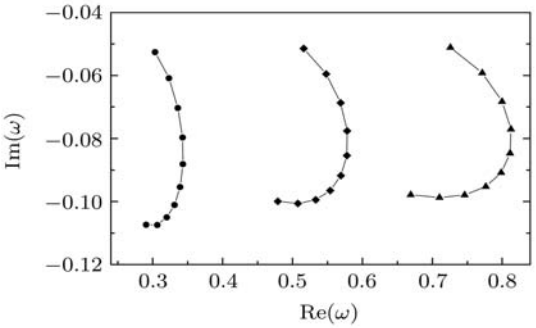


Fig. 7. Variation of real parts and imaginary parts of frequencies of the massless scalar field in LQBH spacetime with parameters $m = 1, a_0 = \sqrt{3}/2$. The behaviour of the frequencies in the complex ω plane shows that the frequencies generally move counterclockwise as the polymeric parameter P increases.

4. Conclusions

We have investigated the dynamical evolution of the massless scalar wave in the LQBH background and numerically studied the complex frequencies of the massless scalar wave. We have found that the polymeric parameter P causes the massless scalar field to decay more quickly and makes the ground scalar wave oscillate slowly. However, the polymeric parameter

P causes the frequency of the high harmonic massless scalar wave shift higher or lower according to the value of polymeric parameter. We have also found that the LQG area gap parameter a_0 causes the massless scalar field to decay more slowly and makes the period of the massless scalar field wave longer. We have found that, in the complex ω plane, the frequency curves move counterclockwise as the polymeric parameter P increases and this spiral effect is more obvious for higher harmonic scalar waves.

References

[1] Rovelli C 2004 *Quantum Gravity* (Cambridge: Cambridge University Press)
[2] Ashtekar A and Lewandowski J 2004 *Class. Quant. Grav.* **21** R53
[3] Han M X, Huang W M and Ma Y G 2007 *Int. J. Mod. Phys.* D **16** 1397
[4] Han M X and Ma Y G 2006 *Class. Quant. Grav.* **23** 2741
[5] Bojowald M 2001 *Phys. Rev. Lett.* **86** 5227
[6] Ashtekar A, Pawlowski T, Singh P and Vandersloot K 2007 *Phys. Rev.* D **75** 024035
[7] Modesto L 2004 *Phys. Rev.* D **70** 124009
[8] Ashtekar A and Bojowald M 2006 *Class. Quant. Grav.* **23** 391
[9] Modesto L 2006 *Class. Quant. Grav.* **23** 5587
[10] Modesto L 2010 *Int. J. Theor. Phys.* arXiv:0811.2196 [gr-qc]
[11] Modesto L 2006 *Class. Quant. Grav.* **23** 5587
[12] Hossenfelder S, Modesto L and Prémont-Schwarz I 2010 *Phys. Rev.* D **81** 044036
[13] Campiglia M, Gambini R and Pullin J 2007 *Class. Quant. Grav.* **24** 3649
[14] Konoplya R A 2003 *Phys. Rev.* D **68** 024018
[15] Maggiore M 2008 *Phys. Rev. Lett.* **100** 141301
[16] Hod S 1998 *Phys. Rev. Lett.* **81** 4293
[17] Dreyer O 2003 *Phys. Rev. Lett.* **90** 081301
[18] Maldacena J 1998 *Adv. Theor. Math. Phys.* **2** 231
[19] Witten E 1998 *Adv. Theor. Math. Phys.* **2** 253
[20] Morgan J, Cardoso V, Miranda A S, Molina C and Zanchin V T 2009 *Phys. Rev.* D **80** 024024
[21] Alsup J and Siopsis G 2008 *Phys. Rev.* D **78** 086001
[22] Cardoso V, Konoplya R and Lemos J P 2003 *Phys. Rev.* D **68** 044024
[23] Jing J L and Pan Q Y 2005 *Nucl. Phys.* B **728** 109
[24] Jing J L 2005 *Phys. Rev.* D **71** 124006
[25] Giammatteo M and Jing J L 2005 *Phys. Rev.* D **71** 024007
[26] Wang B, Lin C Y and Molina C 2004 *Phys. Rev.* D **70** 064025
[27] Du D P, Wang B and Su R K 2004 *Phys. Rev.* D **70** 064024
[28] Ma C R, Gui Y X, Wang W and Wang F J 2006 arXiv: 0611146[gr-qc]
[29] Chakrabarti S K 2007 *Gen. Rel. Grav.* **39** 567
[30] He X, Wang B, Wu S F and Lin C Y 2009 *Phys. Lett.* B **673** 156
[31] Yun S M, Kim Y W and Park Y J 2008 *Eur. Phys. J.* C **58** 617
[32] Chen S B and Jing J L 2005 *Class. Quant. Grav.* **22** 4651
[33] Zhang Y, Gui Y X, Yu F and Li F L 2007 *Gen. Rel. Grav.* **39** 1003
[34] Zhang Y and Gui Y X 2006 *Class. Quant. Grav.* **23** 6141
[35] Xi P 2009 *Astrophys. Space Sci.* **321** 47
[36] Zhang Y, Gui Y X and Yu F 2009 *Chin. Phys. Lett.* **26** 030401
[37] Chen J H and Wang Y J 2010 *Int. J. Mod. Phys.* A **25** 1439
[38] Chen J H and Wang Y J 2003 *Class. Quantum. Grav.* **20** 3897
[39] Chen J H and Wang Y J 2008 *Chin. Phys.* B **17** 1184
[40] Chen J H and Wang Y J 2006 *Chin. Phys.* **15** 1705
[41] Chen J H and Wang Y J 2007 *Chin. Phys.* **16** 3212
[42] Chen J H and Wang Y J 2010 *Chin. Phys.* B **19** 010401
[43] Chen J H and Wang Y J 2010 *Chin. Phys.* B **19** 060401
[44] López-Ortega A 2009 *Int. J. Mod. Phys.* D **18** 1441
[45] Chakrabarti S K 2009 *Eur. Phys. J.* C **61** 477
[46] Kao H C and Tomino D 2008 *Phys. Rev.* D **77** 127503
[47] Cardoso V, Lemos J P S and Yoshida S 2004 *Phys. Rev.* D **69** 044004
[48] Cardoso V, Lemos J P S and Yoshida S 2003 *JHEP* **0312** 004
[49] Jing J L 2005 *JHEP* **0512** 005
[50] Shu F W and Shen Y G 2005 *Phys. Lett.* B **614** 195
[51] Berti E and Kokkotas K D 2003 *Phys. Rev.* D **67** 064020
[52] Brown E, Mann R and Modesto L 2010 arXiv: 1006.4164 [gr-qc]
[53] Schutz B F and Will C M 1985 *Astrophys. J. Lett.* **291** L33
[54] Iyer S and Will C M 1987 *Phys. Rev.* D **35** 3621
[55] Iyer S 1987 *Phys. Rev.* D **35** 3632